

Poly (I:C) and hyaluronic acid directly interact with NLRP3, resulting in the assembly of NLRP3 and ASC in a cell-free system

European Journal of Inflammation
2017, Vol. 15(2) 85–97
© The Author(s) 2017
Reprints and permissions:
sagepub.co.uk/journalsPermissions.nav
DOI: 10.1177/1721727X17711047
journals.sagepub.com/home/eji

Naoe Kaneko,¹ Yuki Ito,¹ Tomoyuki Iwasaki,¹ Hiroyuki Takeda,² Tatsuya Sawasaki,² Kiyoshi Migita,³ Kazunaga Agematsu,⁴ Tomohiro Koga,^{5,6} Atsushi Kawakami,⁵ Akihiro Yachie,⁷ Koh-ichiro Yoshiura,⁸ Shinnosuke Morikawa,¹ Mie Kurata¹ and Junya Masumoto¹

Abstract

In the NLR family, pyrin domain containing 3 (NLRP3) is an intracellular pattern recognition receptor that activates pro-caspase-1, leading to IL-1 β and IL-18 processing and activation in a large complex called the NLRP3 inflammasome. Since various pathogens or endogenous metabolites have been reported to stimulate NLRP3 inflammasome, the interaction between NLRP3 and ASC induced by these stimulants may be an attractive drug target for NLRP3-related diseases, called inflammasomopathies. However, the endogenous ligand that directly interacts with NLRP3, leading to binding to ASC, remains unclear. Therefore, we developed a cell-free system consisting of NLRP3, ASC, and pro-caspase-1 or ASC and NLRP3 with an amplified luminescent proximity homogeneous assay (ALPHA). ALPHA signals of the interaction between NLRP3 and ASC were not enhanced following an incubation without any ligand, whereas strong ALPHA signals for the interaction between NLRP3 and ASC and between NLRP3 and pro-caspase-1 with the adaptor ASC were observed upon an incubation with poly (I:C) and hyaluronic acid (HA). Poly (I:C) and HA both directly interacted with NLRP3 within a specific concentration. These results suggest that NLRP3 directly interacts with intrinsic RNA and HA, which is followed by the activation of NLRP3 inflammasome, and the cell-free system consisting of NLRP3 and ASC, or NLRP3, ASC, and pro-caspase-1 may be a useful tool for elucidating the pathogenesis of inflammasomopathies and developing target therapeutics.

Keywords

ASC, glycosaminoglycan, hyaluronic acid, inflammasome, innate immunity, NLRP3, poly (I:C)

Date received: 10 September 2016; accepted: 26 April 2017

¹Department of Pathology, Proteo-Science Center and Graduate School of Medicine, Ehime University, Toon, Japan

²Division of Cell-Free Sciences, Proteo-Science Center, Ehime University, Matsuyama, Japan

³Department of Gastroenterology and Rheumatology, School of Medicine, Fukushima Medical University, Fukushima, Japan

⁴Department of Infectious Immunology, Graduate School of Medicine, Shinshu University, Matsumoto, Japan

⁵Unit of Translational Medicine, Department of Immunology & Rheumatology, Graduate School of Biomedical Sciences, Nagasaki University, Nagasaki, Japan

⁶Medical Education Development Center, Nagasaki University Hospital, Nagasaki, Japan

⁷Department of Pediatrics, School of Medicine, Institute of Medical, Pharmaceutical and Health Sciences, Kanazawa University, Kanazawa, Japan

⁸Department of Human Genetics, Graduate School of Biomedical Sciences, Nagasaki University, Nagasaki, Japan

Corresponding author:

Junya Masumoto, Department of Pathology, Proteo-Science Center and Graduate School of Medicine, Ehime University, Shitsukawa 454, Toon 791-0295, Ehime, Japan.

Email: masumoto@m.ehime-u.ac.jp



Introduction

In the NLR family, pyrin domain containing 3 (NLRP3), also known as cryopyrin, is an intracellular pattern recognition receptor that is activated by the recognition of pathogen-associated molecular pattern molecules (PAMPs) and/or danger-associated molecular pattern molecules (DAMPs).¹ Activated NLRP3 interacts with the adaptor protein ASC to yield inflammasome, which activate pro-caspase-1, leading to IL-1 β processing and activation in a large complex.^{2,3}

NLRP3 mutations are known to cause an inherited autoinflammatory syndrome, cryopyrin-associated periodic syndrome (CAPS), including Muckle-Wells syndrome (MWS), familial cold autoinflammatory syndrome (FCAS), and neonatal-onset multisystem inflammatory disease (NOMID). CAPS is caused by constitutive active mutations in NLRP3 leading to caspase-1 activation, which results in a high IL-1 β concentration in serum without any PAMPs or DAMPs.^{4,5} NLRP3 has also been implicated in the pathogenesis of metabolic diseases, including type 2 diabetes, atherosclerosis, obesity, and gout.^{6,7} Furthermore, the role of NLRP3 in diseases has been expanded to those of the central nervous system, lungs, liver, and kidney as well as aging.^{8–11} These diseases are considered to be caused by endogenous metabolites. These inflammasome-related disorders are currently referred to as inflammasomopathies.¹²

Various pathogens or danger metabolites have been reported to be recognized by NLRP3, including muramyl dipeptide (MDP), a bacterial cell-wall component; polyinosinic-polycytidylic acid poly (I:C), a virus component; β -amyloid, a misfolded endogenous protein; and uric acid (UA) and ATP; endogenous danger metabolites, with numerous other materials being identified as NLRP3 stimulants.^{4,13–24} However, the endogenous ligand that directly interacts with NLRP3 has not yet been identified in cell cultures or animal models.

These findings prompted us to develop a cell-free system consisting of NLRP3 and ASC, or NLRP3, ASC, and pro-caspase-1 in order to identify ligands that directly activate NLRP3 inflammasome. Although recombinant NLRP3 is difficult to synthesize due to its insolubility, and misfolding occurs when using those from bacteria, yeast, baculo-virus inserts, and mammalian cells, wheat germ cell-free protein synthesis is considered to

overcome this issue in the case of AIM2 inflammasome in a cell-free system.²⁵

In the present study, we demonstrated the synthesis of recombinant NLRP3, ASC, pro-caspase-1, and their truncated forms using a wheat germ cell-free system and identified the endogenous molecules directly interacting with NLRP3.

Materials and methods

Plasmid construction and wheat germ cell-free protein synthesis

The entire cDNA of human ASC was derived from pcDNA3-ASC (accession number: AB023416).²⁶ The entire cDNA of human NLRP3 was derived from a human EST clone (accession number: FLJ95925AAAF). The entire cDNA of human pro-caspase-1 was derived from a human EST clone (accession number: FLJ94074AAAF). The entire cDNA of human IL-1 β was derived from a human EST clone (accession number: FLJ80228AAAN). The entire cDNA of human IL-18 was derived from a human EST clone (accession number: AB590988).

The EST clone coding human NLRP3 was sequenced and two mutations were found: nucleotide sequence 1302C to T resulted in no amino acid change, and nucleotide sequence 1561A to G resulted in an amino acid sequence change from 521M to V. The open reading frame of NLRP3 without a stop codon was modified in a two-step polymerase chain reaction using the following primer sets:

The forward primer S1-NLRP3_F: 5'-CCACCACCACCACCAATGGCAAGCACCCGCTGC-3' with the reverse primer NLRP3-V521M_R: 5'-CTCCTGGAAAGTCATGTGGATGAAGCT-3', and the forward primer NLRP3-V521M_F: 5'-AGCTTCATCCACATGACTTTCCAGGAG-3' with the reverse primer NLRP3-T1(F)_R5'-TCCAGCACTAGCTCCAGACCAAGAAGGCTCAAAGACGACG-3' for the first-step overlapping DNA fragment set, and S1-NLRP3_F with NLRP3-T1(F)_R for the complete version of full-length NLRP3 (NLRP3-FL). Each open reading frame without a stop codon was amplified in polymerase chain reactions as follows: the PCR product was amplified using the primers S1-NLRP3_F with NLRP3(PYD)-T1(F)_R: 5'-TCCAGCACTAGCTCCAGACGGCTCATCTCTTTTGGCTTTC-3' for truncated pyrin domain-only NLRP3 (NLRP3-PYD) (1-90AA).

The EST clone coding human pro-caspase-1 was sequenced and one mutation was detected: nucleotide sequence 539C to T resulted in an amino acid sequence change from 180T to I. The open reading frame of pro-caspase-1 without a stop codon was modified in a two-step polymerase chain reaction using the following primer sets:

The forward primer S1-CASP1_F: 5'-CCACC ACCACCACCAATGGCCGACAAGGT CCTGAA-3' with the reverse primer CASP1 I180T_R: 5'-TCAACCTCAGCTCCAGTTCTT CTAGGAATA-3', and the forward primer CASP1 I180T_F: 5'-TATTCCTAGAAGAACTGGAG CTGAGGTTGA-3' with the reverse primer CASP1-T1(F)_R: 5'-TCCAGCACTAGCTCCAGA ATGTCCTGGGAAGAGGTAGAAAC-3' for the first-step overlapping DNA fragment set, and S1-CASP1_F with CASP1-T1(F)_R for the complete version of full-length pro-caspase-1 (pro-CASP1-FL).

The EST clone coding human IL-1 β was sequenced and one mutation was detected: nucleotide sequence 315T to C resulted in no amino acid change.

Each open reading frame without a stop codon was amplified in polymerase chain reactions. The first-step PCR product was amplified using the primers S1-CASP1_F: 5'-CCACCCACCACCAC CAATGGCCGACAAGGTCCTGAA-3' and CAS P1T1(F)_R: 5'-TCCAGCACTAGCTCCAGAA T G T C C T G G G A A G A G G T A G A AAC-3' for full-length pro-caspase-1 (pro-CASP1-FL); S1-IL-1 β _F: 5'-CCACCCACCACCACC AATGGCAGAAGTACCTGAGCTC-3' and IL-1 β -T1(F)-R: 5'-TCCAGCACTAGCTCCAGAGG AAGACACAAATTGCATGGTGAA-3' for full-length pro-IL-1 β (pro-IL-1 β -FL); S1-IL-18_F: 5'-CCACCCACCACCACCAATGGCTGCTGA ACCAGTAGAA-3' and IL-18-T1(F)-R: 5'-TCCA G C A C T A G C T C C A G A G T C T T C G T T T T GAACAGTGAACATTA-3' for full-length pro-IL-18 (pro-IL-18-FL).

The second step was performed using the following primer sets: attB1-S1: 5'-GGGGAC AAGTTTGTACAAAAAAGCAGGCTT CCACCCACCACCACCAATG-3' and attB2-T1: 5'-GGGGACCACTTTGTACAAGAAAGC TGGGTCTCCAGCACTAGCTCCAGA-3'. These primers are shown in Table 1.

PCR products were inserted into a Gateway™ pDONR™ 221 Vector (pDONR221) (Life

Technologies, Carlsbad, California, USA) using the Gateway™ BP Clonase® II Enzyme mix (Life Technologies, Carlsbad, California, USA) to generate entry clones. The NLRP3 entry clones, pDONR221-NLRP3-FL and pDONR221-NLRP3-PYD, were inserted into pEU-E01-GW-bls-STOP for cell-free protein expression. These constructs were confirmed by sequencing.

The additional truncated NLRP3 entry clones—pDONR221-NLRP3-(Exons 1-2), pDONR221-NLRP3-(Exons 3-9), and pDONR221-NLRP3-(Exons 4-9)—were constructed using the same method with the following primer sets: S1-NLRP3_F with NLRP3(Exons 1-2)-T1(F)_R: T C C A G C A C T A G C T C C A G A T T T C T T C A T T T T A C A A T A G A G A T T C T for pDONR2 21-NLRP3-(Exons 1-2), S1-NLRP3(Exons 3-9)_F: CCACCCACCACCACCAATGGATTACCG TAAGAAGTACAGAAAGTA with NLRP3-T1 (F)_R for pDONR221-NLRP3-(Exons 3-9), and S1-NLRP3(Exons 4-9)_F: CCACCCACCACCAC CAATGGGATTGGTGAACAGCCACCTC with NLRP3-T1(F)_R for pDONR221-NLRP3-(Exons 4-9). These entry clones were inserted into pEU-E01-FLAG-GW-STOP for cell-free protein expression. These constructs were confirmed by sequencing. The above primers are also shown in Table 1.

The ASC entry clones—pDONR221-ASC-FL, pDONR221-ASC-PYD, and pDONR221-ASC-CARD—were constructed as previously reported.²⁵ The additional non-tagged ASC entry clones pDONR221-ASC-FL and full-length pro-caspase-1 entry clones pDONR221-pro-CASP1-FL were inserted into pEU-E01-GW-STOP for cell-free protein expression. The full-length pro-IL-1 β entry clones pDONR221-IL-1 β -FL and full-length pro-IL-18 entry clones pDONR221-IL-18-FL were inserted into pEU-E01-FLAG-GW-Bls-STOP for cell-free protein expression.

The constructed plasmids were used to synthesize specific proteins using a WEPRO1240 Expression Kit (Cell-free, Inc., Matsuyama, Japan) followed by Western blotting.

Western blotting analysis

A total of 1.5 μ g of synthetic protein was subjected to SDS-PAGE followed by a Western blot analysis. Detection on the blotting membranes was performed using anti-FLAG mAb M2

Table 1. Primers used for plasmid construction.

Primer name	Primer sequences
SI-NLRP3_F	5'-CCACCCACCACC CCAATGG CAAGCACCCGCTGC-3'
NLRP3-T1(F)_R	5'-TCCAGCACTAGCTCCAGACCAAGAAGGCTCAAAGACGACG-3'
NLRP3(PYD)-T1(F)_R	5'-TCCAGCACTAGCTCCAGACGGGCTCATCTCTTTTTGCTTTC-3'
NLRP3(Exon1-2)-T1(F)_R	5'-TCCAGCACTAGCTCCAGATTCTTTCATTTTACAAATAGAGATTCT-3'
SI-NLRP3(Exon3-9)_F	5'-CCACCCACCACC CCAATGG ATTACCGTAAGAAGTACAGAAAAGTA-3'
SI-NLRP3(Exon4-9)_F	5'-CCACCCACCACC CCAATGG GATTGGTGAACGCCACCTC-3'
NLRP3-V521M_F	5'-AGCTTCATCCAC AT GTGACTTTCAGGAG-3'
NLRP3-V521M_R	5'-CTCCTGGAAAGT CAT TGTGGATGAAGCT-3'
SI-CASPI_F	5'-CCACCCACCACC CCAATGG CCGACAAGGTCCTGAA-3'
CASPI-T1(F)_R	5'-TCCAGCACTAGCTCCAGAATGTCCTGGGAAGAGGTAGAAAC-3'
CASPI 1180T_F	5'-TATTCCTAGAAGAACTGGAGCTGAGGTTGA-3'
CASPI 1180T_R	5'-TCAACCTCAGCTCCAGTTCTTCTAGGAATA-3'
SI-IL-1 β _F	5'-CCACCCACCACC CCAATGG CAGAAGTACCTGAGCTC-3'
IL-1 β -T1(F)-R	5'-TCCAGCACTAGCTCCAGAGGAAGACACAAATTGCATGGTGAA-3'
SI-IL-18_F	5'-CCACCCACCACC CCAATGG CTGCTGAACCAGTAGAA-3'
IL-18-T1(F)-R	5'-TCCAGCACTAGCTCCAGAGTCTTCGTTTTGAACAGTGAACATTA-3'
attB1-SI	5'-GGGGACAAGTTTGTACAAAAAAGCAGGCTTCCACCCACCACC CCAATG -3'
attB2-T1	5'-GGGGACCACTTTGTACAAGAAAGCTGGGTCTCCAGCACTAGCTCCAGA-3'

Underlined areas indicate SI or T1 sequences. Bold characters indicate Kozak consensus sequences. Italic characters indicate attB1 or attB2 sequences. Bold underlined areas indicate corrected nucleotides.

(Sigma-Aldrich, St. Louis, MO, USA) or Anti-ASC mAb 23-4²⁶ followed by peroxidase-conjugated affinity-purified F(ab')₂ fragments of the goat anti-mouse IgG, F(ab')₂ fragment specific (Jackson ImmunoResearch, West Grove, Pennsylvania, USA) for FLAG-tagged proteins, and non-tagged ASC or HRP-conjugated streptavidin (Nacalai Tesque, Inc., Kyoto, Japan) for biotinylated proteins, respectively.

Amplified luminescent proximity homogeneous assay

Synthesized protein-protein interactions were assessed using the amplified luminescent proximity homogeneous assay (ALPHA). A total of 100 ng of each protein was applied to ALPHA buffer (100 mM Tris-HCl (pH 8.0), 0.01% (v/v) Tween20), 1 mg/mL BSA, 17 μ g/mL streptavidin-conjugated ALPHA donor beads (PerkinElmer, Waltham, Massachusetts, USA), 17 μ g/mL protein-A-conjugated ALPHA acceptor beads, and 5 μ g/mL anti-FLAG mAb M2, and incubated in an ALPHAplate-384 shallow well (PerkinElmer, Waltham, Massachusetts, USA) at 25°C for 24 h. The fluorescence emission signals of each well were measured using an EnSpire™ Multimode Plate Reader (PerkinElmer, Waltham, Massachusetts, USA).

Agarose gel electrophoresis of hyaluronic acid

Agarose gel electrophoresis of hyaluronic acid (HA) was performed according to previously described methods with minor modifications.^{27,28} Briefly, 1.2 μ g of HA standards (Select-HA™ LoLadder, Sigma-Aldrich, St. Louis, Missouri, USA) and 2.4 μ g of each HA sample in 12 μ L of water and 3 μ L of loading buffer was applied to a 1.2% agarose gel. Electrophoresis was performed at room temperature at a current voltage of 25 V for 2 h. After the run, the loaded gel was stained with 0.005% (v/v) Stain-All (Sigma-Aldrich, St. Louis, Missouri, USA) in 50% (v/v) ethanol for 48 h with a cover to protect against light. In destaining, the gel was transferred to 20% ethanol for 24 h.

Pull-down assay

One microgram of C-terminal biotinylated-NLRP3-FL (NLRP3-FL-Btn) and 1 μ g of N-terminal FLAG-tagged ASC-FL (FLAG-ASC-FL) lysed in 300 μ L NP-40 buffer (1% Nonidet P-40, 142.5 mmol/L KCl, 5 mmol/L MgCl₂, 10 mmol/L HEPES (pH 7.6), 0.2 mmol/L phenylmethylsulfonyl fluoride (PMSF), and 1 mmol/L EDTA) were precipitated with 20 μ L streptavidin-conjugated agarose beads (Invitrogen, Grand Island, New York, USA) with or without poly (I:C) or HA, and incubated at 4°C for

3 h. The precipitates were subjected to SDS-PAGE and immunoblotting. Detection on blotting membranes was performed using anti-FLAG mAb M2 or HRP-conjugated streptavidin.

Endotoxin quantification in poly (I:C) and HA

The levels of endotoxin contamination in poly (I:C) and HA were quantified by a Limulus amoebocyte lysate assay using Endospecy, a chromogenic endotoxin-specific assay kit, according to the manufacturer's instructions (Seikagaku-Biobusiness, Tokyo, Japan). An equivalent standard lipopolysaccharide (LPS) was from *Escherichia coli* O55:B5, purified by phenol extraction (L2880), and purchased from Sigma-Aldrich.

Chemicals

MDP (Cat. No. A9519), LPS (Cat. No. L2880), ATP (Cat. No. A2383), UA (Cat. No. U2625), 8-oxo-dG (Cat. No. H5653), aluminum hydroxide (Cat. No. 239186), calcium pyrophosphate (Cat. No. 401552), sodium palmitate (Cat. No. P9767), imiquimod (Cat. No. I5159), poly (I:C) (Cat. No. P1530), poly I (Cat. No. P4154), poly C (Cat. No. P4903), HA-VL (8–15 kDa) (Cat. No. 40583), HA-L (130–150 kDa) (Cat. No. 75043), and HA (700 kDa~) biotin (Cat. No. B1557) were purchased from Sigma-Aldrich. D(+)-glucose (Cat. No. 047-00592) and cholesterol (Cat. No. 034-03002) were purchased from Wako Pure Chemical Industries Ltd. (Osaka, Japan). β -amyloid (Cat. No. AS-20276) was purchased from AnaSpec (Fremont, California, USA). Silica (Cat. No. tlr1-sio), monosodium urate (MSU) (Cat. No. tlr1-msu), Nigericin (Cat. No. tlr1-nig), and poly (I:C) (HMW) biotin (Cat. No. tlr1-picb) were purchased from InVivoGen (San Diego, CA, USA). HA-SVL (2–8 kDa) (Cat. No. NaHA-V2) was purchased from PG Research Inc. (Tokyo, Japan).

Results

Recombinant protein synthesis using a wheat germ cell-free system

NLRP3-FL-Btn and NLRP3-PYD-Btn, FLAG-ASC-FL, pyrin domain-only ASC (FLAG-ASC-PYD), and CARD domain-only ASC (FLAG-ASC-CARD) are schematically presented in Figure 1(a).

Using wheat germ cell-free system-specific expression plasmids, as described previously, FLAG-ASC-FL, FLAG-ASC-CARD, and FLAG-ASC-PYD proteins were synthesized in the same manner as reported²⁵ (Figure 1(b)). NLRP3-FL-Btn and NLRP3-PYD-Btn proteins were successfully synthesized using the wheat germ cell-free system (Figure 1(c)).

Neither MDP nor ATP induced interactions between NLRP3 and ASC in a cell-free system

No significant ALPHA signals of an interaction between FLAG-ASC-FL and NLRP3-FL-Btn were detected upon incubation with 5 mg/mL MDP, which is another NLR Nod2 ligand (Figure 1(d)). No significant ALPHA signals of an interaction between FLAG-ASC-FL and NLRP3-FL-Btn were detected upon an incubation with 5 mg/mL ATP (Figure 1(d)), which was previously reported to be an NLRP3-stimulating ligand in living cells.¹⁸ As positive ALPHA controls, stronger ALPHA signals with no stimulants were detected for NLRP3-FL-Btn with FLAG-ASC-PYD and NLRP3-PYD-Btn with FLAG-ASC-PYD than for the negative control, but not with FLAG-ASC-CARD (Figure 1(d)).

Poly (I:C) and HA induced interactions between NLRP3 and ASC in a cell-free system

Since ATP and MDP did not induce an interaction between NLRP3 and ASC (Figure 1(d)), we investigated whether several materials that were previously reported to be NLRP3 stimulants induced interactions between NLRP3 and ASC. Since ALPHA signals were slightly different in each well, we increased the sample size to five. We used a combination between NLRP3-FL and ASC-PYD with no materials as a positive control, and combinations between NLRP3-FL and ASC-CARD or between NLRP3-FL and ASC-FL with no material as a negative control in the experiment, and showed representative results of independent experiments (Figure 2(a)). An ALPHA-positive control, the interaction between NLRP3-FL-Btn and FLAG-ASC-PYD with no materials, was greater than 36,000 counts. When NLRP3-FL-Btn and FLAG-ASC-FL were incubated with several previously reported NLRP3 stimulants such as 5 mg/mL MDP, 5 mg/mL ATP, 5 mg/mL D(+)-glucose, and solubility-saturated crystals including UA, MSU, 8-oxo-dG, nigericin, cholesterol, silica, aluminum

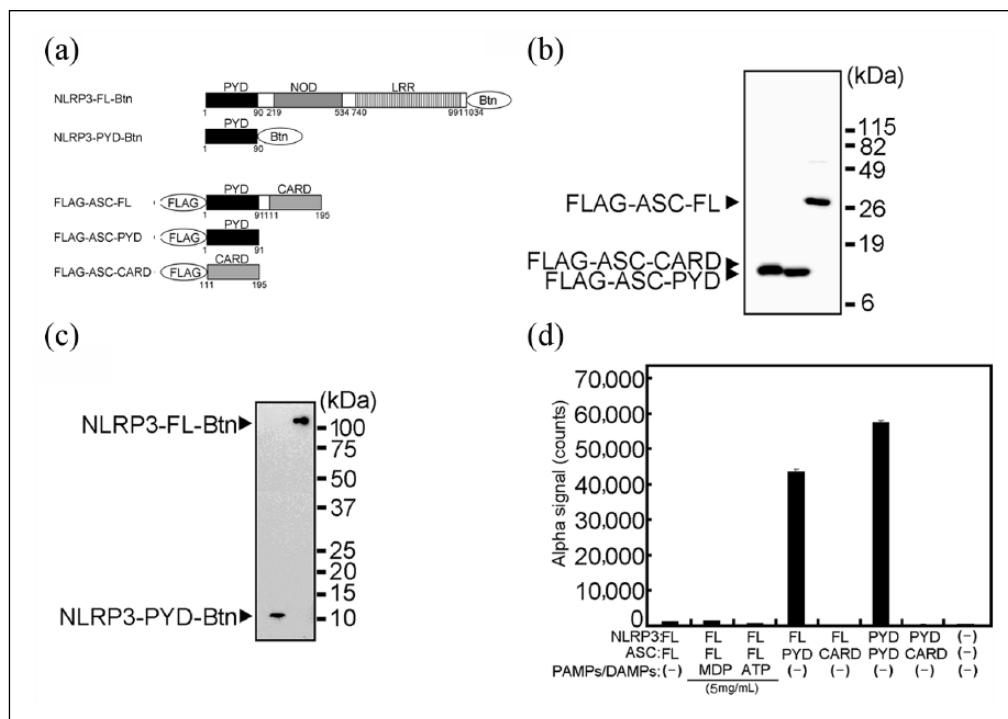


Figure 1. Construction of a cell-free system consisting of ASC and NLRP3. (a) Schematic representations of biotinylated NLRP3 and FLAG-tagged ASC. NLRP3-FL-Btn and NLRP3-PYD-Btn, FLAG-ASC-FL, FLAG-ASC-PYD, and FLAG-ASC-CARD are indicated. The pyrin domain (PYD) is indicated by black boxes. The caspase recruitment domain (CARD) is indicated by light gray boxes. The nucleotide-binding oligomerization domain (NOD) is indicated by dark gray boxes. Leucine-rich repeats are indicated by striped boxes. The amino acid sequence number is indicated under each schema. (b) Wheat germ cell-free synthesis of ASC. A total of 1.5 μ g of synthetic protein was subjected to SDS-PAGE followed by Western blotting. Detection on blotting membranes was performed using anti-FLAG mAb M2 followed by HRP-conjugated affinity-purified F(ab')₂ fragments of goat anti-mouse IgG for FLAG-tagged proteins (b) or HRP-conjugated streptavidin (c). (d) Synthetic protein-protein interactions were detected by ALPHA. Responses (counts) were measured using an EnSpire™ Multimode Plate Reader. Results are representative of three independent experiments and given as the mean \pm standard deviation from triplicate wells.

hydroxide, calcium pyrophosphate, sodium palmitate, β -amyloid, and imiquimod, ALPHA signals were not more than 1000 counts (Figure 2(a)). Among those tested in the present study, ALPHA signals were stronger than 1000 counts in an incubation with 5 mg/mL poly (I:C) and 5 mg/mL HA (Figure 2(a)).

Since previous studies reported that poly (I:C) and HA stimulate NLRP3 inflammasome in cell-based and animal models,^{14,20} we confirmed whether a larger amount of poly (I:C) or different molecular-weight HA induces an interaction between FLAG-ASC-FL and NLRP3-FL-Btn (Figures 2(b)–(e)). ALPHA signals of the interaction between FLAG-ASC-FL and NLRP3-FL-Btn were markedly stronger with 13 mg/mL poly (I:C) than with 5 mg/mL poly (I:C) (Figure 2(a)). As shown in Figure 2(c), poly (I:C) was a mixture of deoxynucleotide chains of approximately 250–1500 bp in size (Figure 2(c)). Regarding HA, ALPHA signals of the interaction between FLAG-ASC-FL and NLRP3-FL-Btn

were markedly stronger with 5 mg/mL of low-molecular-weight HA (HA-L) than with 5 mg/mL of very-low-molecular-weight HA (HA-VL) (Figure 2(d)). HA-VL and HA-L were mixtures of negatively charged glycosaminoglycans of approximately 8–15 kDa and 130–150 kDa in size, respectively (Figure 2(e)).

The interaction between NLRP3-FL-Btn and FLAG-ASC-FL with poly (I:C) or HA was confirmed by immunoprecipitation. FLAG-ASC-FL was co-precipitated with NLRP3-FL-Btn when incubated with 5 mg/mL poly (I:C), and a larger amount of FLAG-ASC-FL was co-precipitated when incubated with 13 mg/mL poly (I:C) (Figure 2(f)). FLAG-ASC-FL was not co-precipitated with NLRP3-FL-Btn when incubated with no materials or 5 mg/mL HA-SVL (2–8 kDa). FLAG-ASC-FL was weakly co-precipitated when incubated with 5 mg/mL HA-VL, and a larger amount of FLAG-ASC-FL was co-precipitated when incubated with 5 mg/mL HA-L (Figure 2(f)).

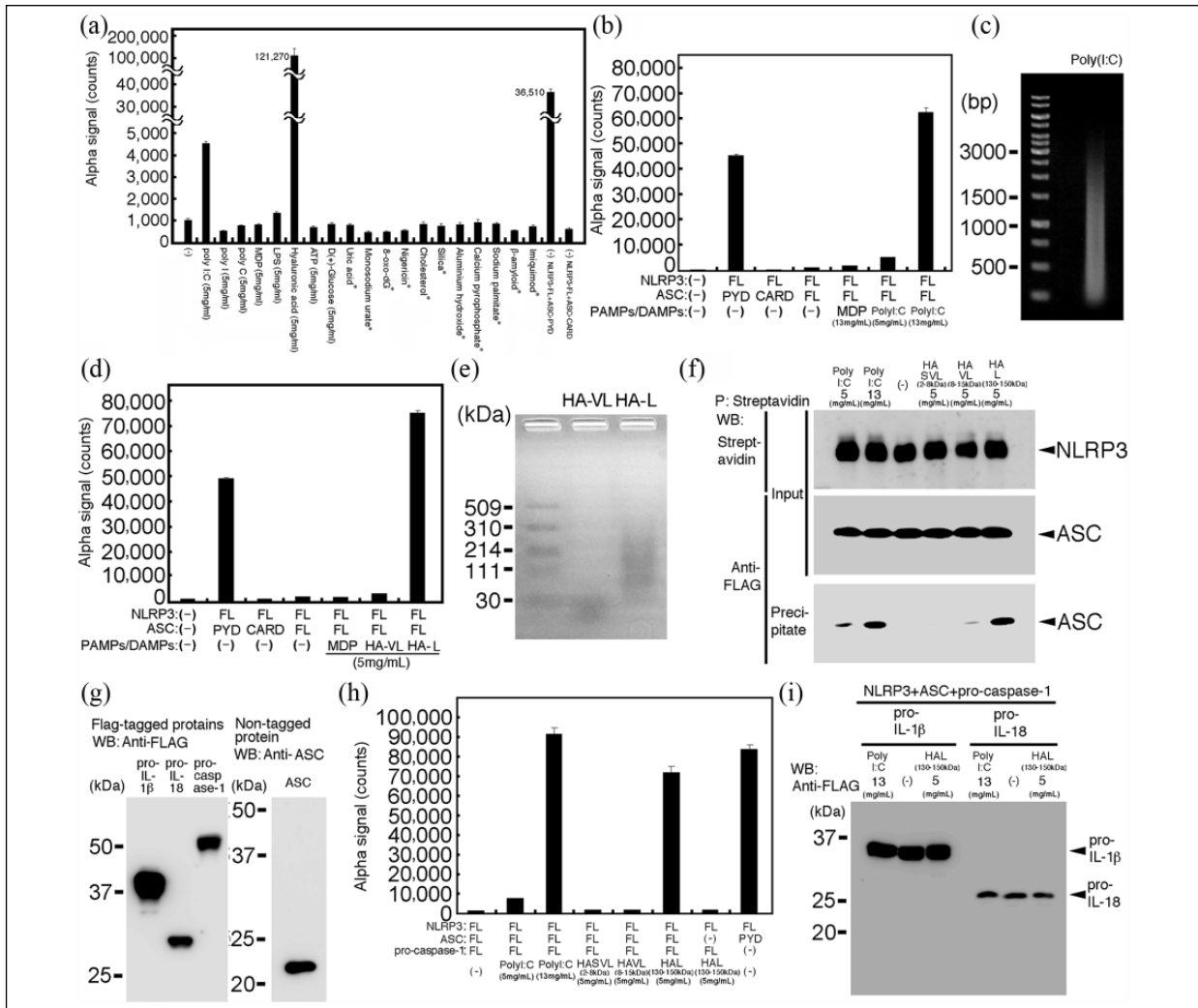


Figure 2. Poly (I:C) and HA induced the assembly of NLRP3, ASC, and pro-caspase-1 in the cell-free system. (a) Possible NLRP3 stimulants were screened. A total of 100ng of each protein indicated was incubated with 5 μg/mL anti-FLAG mAb M2, 17 μg/mL protein-A-conjugated ALPHA acceptor beads, and 17 μg/mL streptavidin-conjugated ALPHA donor beads for 24h with or without the indicated amount of materials. Asterisks indicate solubility-saturated nano-crystals or water-insoluble materials; therefore, concentrations are not indicated. Results are representative of four independent experiments and given as the mean ± standard deviation of five wells. (b) Effects on the assembly of NLRP3 and ASC in a cell-free system by poly (I:C). Positive ALPHA signals were observed with 5mg/mL poly (I:C). Markedly stronger ALPHA signals were observed with 13 mg/mL poly (I:C). The combinations of NLRP3, ASC, and their truncated proteins are indicated. Results are representative of three independent experiments and given as the mean ± standard deviation of triplicate wells. (c) Agarose gel electrophoresis of poly (I:C). A total of 1.3 μg of the poly (I:C) used in the experiment was run on a 1.0% agarose gel and visualized using ethidium bromide. (d) Effects on the assembly of NLRP3 and ASC in a cell-free system by HA. Strong ALPHA signals were observed with 8-15-kDa HA (HA-VL). Markedly stronger ALPHA signals were observed with 130-150-kDa HA (HA-L). The combinations of NLRP3, ASC, and their truncated proteins are indicated. Results are representative of three independent experiments and given as the mean ± standard deviation of triplicate wells. (e) Agarose gel electrophoresis of HA. A total of 2.4 μg of HA-L and HA-VL used in the experiment was run on a 1.2% agarose gel and the loaded gel was stained with 0.005% (v/v) Stain-All. (f) A pull-down assay was performed. A total of 1 μg NLRP3-FL-Btn and 1 μg FLAG-ASC-FL lysed in 300 μl NP-40 buffer were precipitated with 20 μl streptavidin-conjugated agarose beads with or without the indicated amount of poly (I:C) or indicated molecular weight of HA. The precipitates were subjected to SDS-PAGE and immunoblotting. Detection on the blotting membranes was performed using anti-FLAG mAb M2 or HRP-conjugated streptavidin. (g) Wheat germ cell-free synthesis of FLAG-tagged pro-IL-1β, pro-IL-18, pro-CASPI-FL, and non-tagged ASC. A total of 1.5 μg of the synthetic protein was subjected to SDS-PAGE followed by Western blotting. Detection on blotting membranes was performed using anti-FLAG mAb M2 or anti-ASC mAb 23-4 followed by the HRP-conjugated affinity-purified F(ab)₂ fragments of goat anti-mouse IgG. (h) A cell-free system consisting of NLRP3-FL-Btn, non-tagged ASC, and FLAG-tagged pro-CASPI-FL in a cell-free system with ALPHA. A total of 100ng of each protein indicated was incubated with 5 μg/mL anti-FLAG mAb M2, 17 μg/mL protein-A-conjugated ALPHA acceptor beads, and 17 μg/mL streptavidin-conjugated ALPHA donor beads for 24h with or without the indicated amount of materials. (i) The cell-free system did not process pro-IL-1β or pro-IL-18 in a cell-free system. The cell-free system consisting of NLRP3-FL-Btn, non-tagged ASC, and FLAG-pro-CASPI-FL was incubated with 13 mg/mL poly (I:C) or 5mg/mL HA-L for 24h. IL-1β and IL-18 were detected by SDS-PAGE followed by Western blotting. PYD: pyrin domain; CARD: caspase recruitment domain; FL: full length; SVL: Super very low; VL: Very low; L: Low.

Poly (I:C) and HA induced the assembly of NLRP3, ASC, and pro-caspase-1 in a cell-free system

In order to further confirm that poly (I:C) and HA induce the assembly of NLRP3, ASC, and pro-caspase-1, resulting in the processing of pro-IL-1 β and pro-IL-18, we synthesized FLAG-tagged pro-CASP1-FL, FLAG-pro-IL-1 β , FLAG-pro-IL-18, and non-tagged ASC using a wheat germ cell-free system (Figure 2(g)). ALPHA signals of the interaction between FLAG-ASC-FL and NLRP3-FL-Btn with adaptor non-tagged ASC were elevated when incubated with 5 mg/mL poly (I:C) and 13 mg/mL poly (I:C) in a dose-dependent manner, and also with HA-L (Figure 2(h)). However, neither pro-IL-1 β nor pro-IL-18 was processed when incubated with FLAG-NLRP3-FL, non-tagged ASC, and FLAG-pro-CASP1 with 13 mg/mL poly (I:C) or 5 mg/mL HA-L (Figure 2(i)).

Poly (I:C) and HA directly interacted with NLRP3

In order to confirm the direct interaction between NLRP3 and poly (I:C) or between NLRP3 and HA, we examined the interaction between N-terminal FLAG-tagged full-length NLRP3 (FLAG-NLRP3) and biotinylated poly (I:C) or biotinylated HA (Figures 3(a) and (b)). The ALPHA signals of these interactions gradually increased with 1.0 μ g/mL biotinylated poly (I:C), and decreased at higher concentrations of biotinylated poly (I:C) (Figure 3(a)). The ALPHA signals of these interactions gradually increased with 0.1 μ g/mL biotinylated HA, and decreased at higher concentrations of biotinylated HA (Figure 3(b)). We then assessed the specific binding site of NLRP3 with 1.0 μ g/mL biotinylated poly (I:C) or 0.1 μ g/mL biotinylated HA. N-terminal FLAG-tagged NLRP3 truncated proteins—such as FLAG-NLRP3-(Exons 1-2), FLAG-NLRP3-(Exons 3-9), and FLAG-NLRP3-(Exons 4-9)—were prepared (Figure 3(c) and (d)). Stronger ALPHA signals were detected between FLAG-NLRP3-(Exon 3-9) and 1.0 μ g/mL biotinylated poly (I:C) or 0.1 μ g/mL biotinylated HA among FLAG-NLRP3-(Exons 1-2), FLAG-NLRP3-(Exons 3-9), and FLAG-NLRP3-(Exons 4-9) (Figure 3(e) and (f)).

Endotoxin contaminant in HA and poly (I:C)

In order to clarify whether the endotoxin contaminant affects the cell-free system, we measured the amount of the endotoxin contaminant in HA and poly (I:C) using a Limulus amoebocyte lysate assay. As shown in supplementary Table S1, HA-SVL included 11.3 EU/mg endotoxin contaminant equivalent to 1.40 ng/mg LPS from *Escherichia coli* O55:B5 (Sigma-Aldrich L2880) and 53.4 μ g/mg protein. HA-VL included 0.0153 EU/mg endotoxin contaminant equivalent to 1.89 pg/mg LPS from *Escherichia coli* O55:B5 and 22.7 μ g/mg protein. HA-L included 0.222 EU/mg endotoxin contaminant equivalent to 27.4 pg/mg LPS from *Escherichia coli* O55:B5 and 13.0 μ g/mg protein. Poly (I:C) included 8360 EU/mg endotoxin contaminant equivalent to 1.01 μ g/mg LPS from *Escherichia coli* O55:B5 and 5.52 μ g/mg protein. The endotoxin concentrations of each sample were verified. We then tested whether the same equivalent of LPS as the amount of contaminated endotoxin influences the interaction between NLRP3-FL-Btn and FLAG-FL-ASC. The contaminated amount of endotoxin did not appear to influence assembly of NLRP3 and ASC in the cell-free system (Supplementary Figure S1).

Discussion

We herein report the development of a cell-free system consisting of ASC and NLRP3, or NLRP3, ASC, and pro-caspase-1 with ALPHA in order to identify directly stimulating endogenous ligands. Our cell-free system is basically composed of NLRP3 and ASC. Similar functions were observed using a tertiary complex consisting of NLRP3, ASC, and pro-caspase-1 (Figures 1 and 2). These results were consistent with the functions of NLRP3, which recognizes its ligand by LRR and then interacts with the adaptor protein ASC.¹

As a positive control of our system, we attempted to confirm whether the cell-free system consisting of NLRP3 and ASC recognizes ATP, a well-known intrinsic NLRP3 activator.¹⁸ However, the maximum amount of 5 mg/mL ATP or a markedly lower concentration did not elevate ALPHA signals, similar to the negative control (Figure 1(d)). There are at least two possibilities to explain this result: one is that our cell-free system did not function properly, the other is that there are at least one or more mediators activating NLRP3 inflammasome.

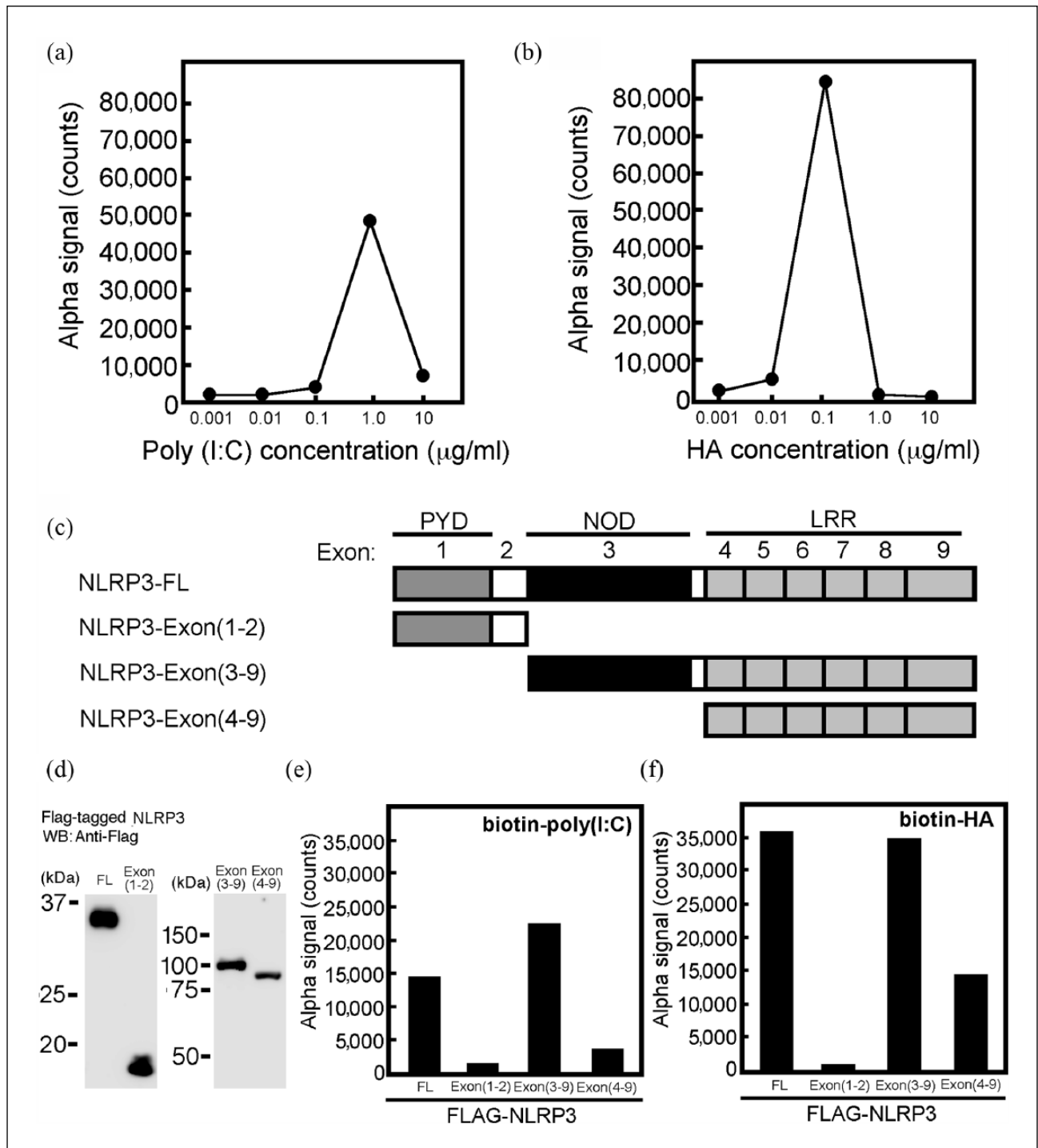


Figure 3. Poly (I:C) and HA directly interact with the NOD-LRR domain of NLRP3 with specific concentrations. (a, b) A peak ALPHA signal of the interaction was observed when 100 ng of FLAG-NLRP3 was incubated with 5 $\mu\text{g/ml}$ anti-FLAG mAb M2, 17 $\mu\text{g/ml}$ protein-A-conjugated ALPHA acceptor beads, and 17 $\mu\text{g/ml}$ streptavidin-conjugated ALPHA donor beads for 24 h with 1.0 $\mu\text{g/ml}$ biotinylated poly (I:C) or 0.1 $\mu\text{g/ml}$ biotinylated HA, respectively. (c) A schematic representation of the NLRP3 structure depicts exon components and truncated proteins. (d) The wheat germ cell-free synthesis of FLAG-NLRP3-FL, FLAG-NLRP3-(Exons 1-2), FLAG-NLRP3-(Exons 3-9), and FLAG-NLRP3-(Exons 4-9) was detected by SDS-PAGE followed by Western blotting. (e) Interactions between 1.0 $\mu\text{g/ml}$ biotinylated poly (I:C) and FLAG-NLRP3-FL, FLAG-NLRP3-(Exons 1-2), FLAG-NLRP3-(Exons 3-9), or FLAG-NLRP3-(Exons 4-9). (f) Interactions between 0.1 $\mu\text{g/ml}$ biotinylated HA and FLAG-NLRP3-FL, FLAG-NLRP3-(Exons 1-2), FLAG-NLRP3-(Exons 3-9), or FLAG-NLRP3-(Exons 4-9).

In order to confirm these possibilities, we screened several previously reported NLRP3-stimulating agents.^{4,13–24} Among the agents tested, poly (I:C) and HA induced elevations in ALPHA signals for the interaction between NLRP3 and ASC (Figure 2(a)). Further experiments confirmed that a different amount of poly (I:C) or different molecular-weight HA induced the interaction between NLRP3 and ASC (Figure 2(b)–(e)). The interaction between NLRP3 and ASC was also confirmed by the pull-down assay (Figure 2(f)). These results are consistent with those shown in Figure 2(a). It is important to note that 2–8-kDa HA-SVL did not induce the interaction between NLRP3-FL-Btn and FLAG-tagged ASC (Figure 2(f)). Thus, the minimum saccharide length that makes precipitated ASC with NLRP3 appears to be approximately 8–15-kDa HA consisting of 20–38 mer of a D-glucuronic acid- β -1,3-D-N-acetyl glucosamine- β -1,4-repeat.

Since the assembly of *in vivo* NLRP3 inflammasome is required for the combination of NLRP3, ASC, and pro-caspase-1, resulting in pro-IL-1 β and pro-IL-18 processing, the detection of an interaction between NLRP3 and ASC does not appear to be sufficient. Therefore, we synthesized FLAG-pro-CASP1-FL, FLAG-pro-IL-1 β , and FLAG-pro-IL-18 and attempted to assess the interaction between NLRP3-FL-Btn and FLAG-pro-CASP1-FL with non-tagged adaptor ASC (Figure 2(g) and (h)). As expected, 13 mg/mL poly (I:C) and 5 mg/mL HA-L strongly induced the assembly of NLRP3, ASC, and pro-caspase-1 (Figure 2(h)). However, the assembly of only NLRP3, ASC, and pro-caspase-1 did not lead to pro-IL-1 β or pro-IL-18 processing (Figure 2(i)).

ATP did not induce the simple assembly of NLRP3 and ASC in a cell-free system (Figures 1 and 2). This finding is consistent with ATP requiring its membranous receptor P2X7 and a reactive oxygen species (ROS) system for the activation of NLRP3 inflammasome in living cells.²⁹ In addition, poly (I:C) and HA induced the assembly of NLRP3, ASC, and pro-caspase-1 in a cell-free system, but had no effect on the processing of IL-1 or IL-18 (Figure 2(i)). These results support poly (I:C) stimulating NLRP3 inflammasome in the presence of mature lysosome and ROS in living cells. Alternatively, poly (I:C) stimulates NLRP3 in the presence of mature lysosome and ROS participation.¹³ Thus, the cell-free system is limited to

reflecting an initial event in the assembly of NLRP3 and ASC only. However, the cell-free system may be a sufficiently useful tool as an assessment system for inflammasome-targeted drugs or assembly inducible ligands. Previous studies reported that caspase-8 may be required for the production of IL-1 β .^{30,31} Thus, we speculated that several extra components are needed for the processing of pro-IL-1 β or pro-IL-18 in addition to pro-caspase-1.

Poly (I:C)—a synthetic analog of the double-stranded RNA (dsRNA) of RNA viruses such as paramyxovirus, influenza virus, and picornavirus—is a pathogen-associated molecular pattern molecule that has been reported to activate NLRP3.¹³ Virus dsRNA is recognized by other types of intracellular pattern recognition receptors: RIG-1-like receptors such as RIG-1, MDA5, and LGP2, via their RNA helicase domains, and activate interferon pathways.³² RNA may be recognized by NLRP3 via a similar mechanism.

HA has also been reported to activate NLRP3 inflammasome.²⁰ HA is a well-known extracellular matrix that is involved in tissue injury, tissue repair, inflammation, cell proliferation, and/or migration. The various functions of HA depend on its size.³³ For example, the expression of inflammatory cytokines is induced by HA fragments in the 1000–1250 saccharide range (200–250 kDa). Markedly smaller HA predominantly induces angiogenesis rather than cytokine release.³³ Consistent with this finding, a stronger ALPHA signal for the interaction between NLRP3 and ASC was induced by HA-L (approximately 130–150 kDa) than by HA-VL (approximately 8–15 kDa) (Figure 2(d) and (e)).

Although previous studies reported that IL-1 β is activated by poly (I:C) or HA, depending on the presence of NLRP3,²⁰ it currently remains unclear whether the interaction between NLRP3 and poly (I:C) or HA is direct or indirect. Since NLRP3 directly interacted with poly (I:C) and HA through the NLRP3-NOD-LRR domain (Figure 3(a)–(e)), our results provide strong evidence for the direct activation of NLRP3 by poly (I:C), an exogenous pathogen, or HA, an endogenous metabolite, without any mediators (Figure 3(a)–(e)).

Strong signals were obtained by poly (I:C) and HA, both of which charged strand-like molecules that are expected to sterically and non-specifically ensnare the cell-free system; therefore, we consider it important for the results obtained to be

confirmed by a more physiological system. However, previous studies demonstrated that poly (I:C) and HA both activated NLRP3 inflammasome.^{13,14,20} Thus, the cell-free system consisting of NLRP3 and ASC may reflect at least an initial event in the activation of inflammasome; however, it has a limitation in regards of the artificial cell-free system.

In view of physiological functions, differences between HA-L and HA-VL result in interactions with different receptors called hyaladherins such as CD44; therefore, the trigger is vastly more complex, particularly in cell-based systems.³⁴ On the other hand, our cell-free system is composed of not more than two or three components. In addition, in the same dose of HA-L and HA-VL by weight, since HA is nothing but a repeat disaccharide sequence, the amount of disaccharides should be identical. The difference between L-HA and VL-HA in the cell-free system appears to depend on the length of the saccharide sequence only. Therefore, we speculate that the mechanism of induction of the interaction between NLRP3 and ASC depends on hanging by the polymer sequence such as a polysaccharide or RNA chain.

In the present study, nano-crystals including UA, silica, aluminum hydroxide, and calcium pyrophosphate did not induce the interaction between NLRP3 and ASC in the cell-free system (Figure 2(a)). Since crystals cannot be digested by cells, similar to a cell-free system, crystals phagocytosed by resident macrophages, via a process termed “frustrated phagocytosis,” are considered to be involved in the production of NADPH oxidase-induced ROS.³⁵ ROS have been reported to degrade high-molecular-weight HA into low-molecular-weight HA.^{36,37} Therefore, we speculate that ROS induce HA degradation and cellular internalization, and HA directly interacts with NLRP3 as an initial event for the activation of NLRP3 inflammasome. Consistent with the above hypothesis, some cases of acute synovitis or arthritis after an intra-articular hyaluronate injection have been reported.³⁸

Poly (I:C) and HA are both involved in wound healing and excess inflammation.^{39,40} Wound healing is known to be promoted by IL-1 β and IL-18, both of which are processed by inflammasomes; however, excess amounts of IL-1 β and IL-18 induce tissue injury. Thus, the regulation of poly (I:C) and HA signaling through NLRP3 inflammasome may be an attractive

therapy to promote wound healing and abrogate excess inflammation.

In conclusion, we herein developed a cell-free system consisting of ASC and NLRP3. NLRP3 inflammasome have been implicated in various disorders, called inflammasomopathies including autoinflammatory diseases.^{4,12} Therefore, the cell-free system developed in the present study may be a useful tool for elucidating the pathogenesis of inflammasomopathies and developing target therapeutics.

Acknowledgements

N.K. and Y.I. contributed equally to this work.

Declaration of conflicting interests

The author(s) declared no potential conflicts of interest with respect to the research, authorship, and/or publication of this article.

Funding

This work was supported by the Platform for Drug Discovery, Informatics and Structural Life Science from the Ministry of Education, Culture, Sports, Science and Technology, Japan (H.T., T.S., and J.M.); the Center for Clinical and Translational Research of Kyushu University (J.M.); a Grant-in-Aid for translational research toward the clarification of autoinflammatory mechanisms by familial Mediterranean fever (FMF) inflammasome based on the Mediterranean fever (*MEFV*) gene analysis 26310301 from The Ministry of Health, Labour and Welfare, Japan (K.M., K.A., T.K., A.K., A.Y., and J.M.); and Grants-in-Aid for Scientific Research (JSPS KAKENHI Grant numbers 26293232, 26305024 and 17H04656) from The Ministry of Education, Culture, Sports, Science and Technology, Japan (J.M.).

References

1. Franchi L, Muñoz-Planillo R and Núñez G (2012) Sensing and reacting to microbes through the inflammasomes. *Nature Immunology* 13: 325–332.
2. Manji GA, Wang L, Geddes BJ et al. (2002) PYPAF1, a PYRIN-containing Apaf1-like protein that assembles with ASC and regulates activation of NF- κ B. *Journal of Biological Chemistry* 277: 11570–11575.
3. Srinivasula SM, Poyet JL, Razmara M et al. (2002) The PYRIN-CARD protein ASC is an activating adaptor for caspase-1. *Journal of Biological Chemistry* 277: 21119–21122.
4. Martinon F, Agostini L, Meylan E et al. (2004) Identification of bacterial muramyl dipeptide as activator of the NALP3/cryopyrin inflammasome. *Current Biology* 14: 1929–1934.

5. Yamazaki T, Masumoto J, Agematsu K et al. (2008) Anakinra improves sensory deafness in a Japanese patient with Muckle-Wells syndrome, possibly by inhibiting the cryopyrin inflammasome. *Arthritis & Rheumatology* 58: 864–868.
6. Kastner DL, Aksentijevich I and Goldbach-Mansky R (2010) Autoinflammatory disease reloaded: A clinical perspective. *Cell* 140: 784–790.
7. Wen H, Ting JP and O’Neill LA (2012) A role for the NLRP3 inflammasome in metabolic diseases—did Warburg miss inflammation? *Nature Immunology* 13: 352–357.
8. Anders HJ and Muruve DA (2011) The inflammasomes in kidney disease. *Journal of the American Society of Nephrology* 22: 1007–1018.
9. Szabo G and Csak T (2012) Inflammasomes in liver diseases. *Journal of Hepatology* 57: 642–654.
10. Youm YH, Grant RW, McCabe LR et al. (2013) Canonical NLRP3 inflammasome links systemic low-grade inflammation to functional decline in aging. *Cell Metabolism* 18: 519–532.
11. De Nardo D, De Nardo CM and Latz E (2014) New insights into mechanisms controlling the NLRP3 inflammasome and its role in lung disease. *American Journal of Pathology* 184: 42–54.
12. Masters SL, Simon A, Aksentijevich I et al. (2009) Horror autoinflammaticus: The molecular pathophysiology of autoinflammatory disease. *Annual Review of Immunology* 27: 621–668.
13. Allen IC, Scull MA, Moore CB et al. (2009) The NLRP3 inflammasome mediates in vivo innate immunity to influenza A virus through recognition of viral RNA. *Immunity* 30: 556–565.
14. Rajan JV, Warren SE, Miao EA et al. (2010) Activation of the NLRP3 inflammasome by intracellular poly I:C. *FEBS Letters* 584: 4627–4632.
15. Halle A, Hornung V, Petzold GC et al. (2008) The NALP3 inflammasome is involved in the innate immune response to amyloid- β . *Nature Immunology* 9: 857–865.
16. Denoble AE, Huffman KM, Stabler TV et al. (2011) Uric acid is a danger signal of increasing risk for osteoarthritis through inflammasome activation. *Proceedings of the National Academy of Sciences of the United States of America* 108: 2088–2093.
17. Martinon F, Pétrilli V, Mayor A et al. (2006) Gout-associated uric acid crystals activate the NALP3 inflammasome. *Nature* 440: 237–241.
18. Mariathasan S, Weiss DS, Newton K et al. (2006) Cryopyrin activates the inflammasome in response to toxins and ATP. *Nature* 440: 228–232.
19. Franchi L, Eigenbrod T, Muñoz-Planillo R et al. (2009) The inflammasome: A caspase-1-activation platform that regulates immune responses and disease pathogenesis. *Nature Immunology* 10: 241–247.
20. Yamasaki K, Muto J, Taylor KR et al. (2009) NLRP3/cryopyrin is necessary for interleukin-1 β (IL-1 β) release in response to hyaluronan, an endogenous trigger of inflammation in response to injury. *Journal of Biological Chemistry* 284: 12762–12771.
21. Rajamäki K, Lappalainen J, Oörni K et al. (2010) Cholesterol crystals activate the NLRP3 inflammasome in human macrophages: A novel link between cholesterol metabolism and inflammation. *PLoS ONE* 5: e11765.
22. Kanneganti TD, Ozören N, Body-Malapel M et al. (2006) Bacterial RNA and small antiviral compounds activate caspase-1 through cryopyrin/Nalp3. *Nature* 440: 233–236.
23. Shimada K, Crother TR, Karlin J et al. (2012) Oxidized mitochondrial DNA activates the NLRP3 inflammasome during apoptosis. *Immunity* 36: 401–414.
24. Zhou R, Tardivel A, Thorens B et al. (2010) Thioredoxin-interacting protein links oxidative stress to inflammasome activation. *Nature Immunology* 11: 136–140.
25. Kaneko N, Ito Y, Iwasaki T et al. (2015) Reconstituted AIM2 inflammasome in cell-free system. *Journal of Immunological Methods* 426: 76–81.
26. Masumoto J, Taniguchi S, Ayukawa K et al. (1999) ASC, a novel 22-kDa protein, aggregates during apoptosis of human promyelocytic leukemia HL-60 cells. *Journal of Biological Chemistry* 274: 33835–33838.
27. Lee HG and Cowman MK (1994) An agarose gel electrophoretic method for analysis of hyaluronan molecular weight distribution. *Analytical Biochemistry* 219: 278–287.
28. Cowman MK, Chen CC, Pandya M et al. (2011) Improved agarose gel electrophoresis method and molecular mass calculation for high molecular mass hyaluronan. *Analytical Biochemistry* 417: 50–56.
29. Cruz CM, Rinna A, Forman HJ et al. (2007) ATP activates a reactive oxygen species-dependent oxidative stress response and secretion of proinflammatory cytokines in macrophages. *Journal of Biological Chemistry* 282: 2871–2879.
30. Man SM, Toulomousis P, Hopkins L et al. (2013) Salmonella infection induces recruitment of Caspase-8 to the inflammasome to modulate IL-1 β production. *Journal of Immunology* 191: 5239–5246.
31. Philip NH, Dillon CP, Snyder AG et al. (2014) Caspase-8 mediates caspase-1 processing and innate immune defense in response to bacterial blockade of NF- κ B and MAPK signaling. *Proceedings of the National Academy of Sciences of the United States of America* 111: 7385–7390.
32. Kawai T and Akira S (2009) The roles of TLRs, RLRs and NLRs in pathogen recognition. *International Immunology* 21: 317–337.

33. Stern R, Asari AA and Sugahara KN (2006) Hyaluronan fragments: An information-rich system. *European Journal of Cell Biology* 85: 699–715.
34. Knudson CB and Knudson W (1993) Hyaluronan-binding proteins in development, tissue homeostasis, and disease. *FASEB Journal* 7: 1233–1241.
35. Joshi S, Wang W, Peck AB et al. (2015) Activation of the NLRP3 inflammasome in association with calcium oxalate crystal induced reactive oxygen species in kidneys. *Journal of Urology* 193: 1684–1691.
36. Esser PR, Wölfle U, Dürr C et al. (2012) Contact sensitizers induce skin inflammation via ROS production and hyaluronic acid degradation. *PLoS ONE* 7: e41340.
37. Hu Y, Mao K, Zeng Y et al. (2010) Tripartite-motif protein 30 negatively regulates NLRP3 inflammasome activation by modulating reactive oxygen species production. *Journal of Immunology* 185: 7699–7705.
38. Wendling D, Royer F, Chabroux A et al. (2007) Acute gouty arthritis after intraarticular hyaluronate injection. *Joint Bone Spine* 74: 664–665.
39. Sidhu GS, Thaloor D, Singh AK et al. (1996) Enhanced biosynthesis of extracellular matrix proteins and TGF- β 1 by polyinosinic-polycytidylic acid during cutaneous wound healing in vivo. *Journal of Cellular Physiology* 169: 108–114.
40. Artlett CM (2013) Inflammasomes in wound healing and fibrosis. *Journal of Pathology* 229: 157–167.